Iğdır Üniversitesi Fen Bilimleri Enstitüsü Dergisi, 13(3), 1946-1957, 2023
Journal of the Institute of Science and Technology, 13(3), 1946-1957, 2023
ISSN: 2146-0574, eISSN: 2536-4618

Chemistry **DOI: 10.21597/jist.1275258**

Research Article

Received: 01.04.2023 **Accepted: 25.05.2023**

To Cite: Kucuk, I., Gözcü, M. (2023). Removal of Crystal Violet From Aqueous Solutions by A Newly Developed Adsorbent: İsotherm, Kinetics, and Thermodynamics. *Journal of the Institute of Science and Technology*, 13(3), 1946-1957.

Removal of crystal Violet From Aqueous Solutions by A Newly Developed Adsorbent: İsotherm, Kinetics, and Thermodynamics

Ilhan KUÇUK[1*] Merve GOZCU[2]

Highlights:

- Removal of crystal violet
- Adsorbent characterization
- 3 different modifications
- Isotherm kinetic and thermodynamic studies

Keywords:

- Watermelon Peel
- Agricultural Waste
- Characterization
- Adsorption
- Crystal Violent

ABSTRACT:

Aim of this study, adsorption potential of modified and natural materials is investigated. The adsorbent used is watermelon peel (WP) derived from agricultural wastes to remove crystal violet (CV). The modified and raw adsorbent was characterized by Elemental analysis, Scanning electron microscope (SEM), X-ray diffraction (XRD), and Fourier transform infrared spectroscopy (FTIR). The studied parameters are temperature, initial metal concentration, and contact time. The most suitable kinetic (R^2=0.99) and isotherm (R^2=0.99) models were determined as Pseudo-second-order and Langmuir, respectively. The maximum adsorption capacity (qmax) according to Langmuir is 236.9 mg/g at 30°C. Thermodynamic analysis revealed spontaneous and endothermic adsorption of CV on modified watermelon peels. These results demonstrate that crystal violet can be removed from agricultural wastes using a low-cost adsorbent.

[1] Ilhan KUCUK (**Orcid ID:** 0000-0003-2876-3942), Rectorship, Muş Alparslan University, Muş, Türkiye
[2] Merve GOZCU (**Orcid ID:** 0009-0004-2355-9867), Technıcal Scıences Vocatıonal School, Muş Alparslan University, Muş, Türkiye

[*]**Corresponding Author:** Ilhan KUCUK, e-mail: i.kucuk@alparslan.edu.tr

INTRODUCTION

Significant environmental problems occur when toxic constituents from industrial and agricultural activities proliferate uncontrollably in soil and water. The receiving environment, into which wastewater is discharged without treatment, may be contaminated with various pollutants such as acidic and basic substances, toxic organic substances, inorganic substances, and heavy metals (Öter, 2021). In particular, solids and dyes produced in the textile industry are among the important pollutant industries, as they disturb the ecological balance and cause serious problems (Kul et al., 2019). One of these dyes is crystal violet, which is usually in the form of sodium salt. Its general formula is $C_{25}H_{30}N_3Cl$. It is mainly used for dyeing nylon and wool in the textile industry (Bayram et al., 2023). In general, wastewater containing dye has high pH, strong color, low biodegradability and high chemical oxygen demand (Güneş, 2020). Therefore, the color must be removed from the contaminated water before it is discharged. Many methods such as coagulation, anaerobic and aerobic microbial degradation, adsorption, membrane separation processes, chemical oxidation, electrochemical separation, flotation, dilution, filtration and reverse osmosis are used for color removal. Among these methods, adsorption is considered one of the most sustainable approaches for removing dyes due to the simplicity of design, economic viability, high efficiency, and environmentally benign nature (Dinçer et al., 2019, Gürsel et al., 2021).

Activated carbon is an effective adsorbent commonly used to remove dyes, and adsorption remains the leading treatment method. However, some problems occur when using activated carbon (Heidarinejad et al., 2020). Activated carbon is of higher quality, an expensive product and a higher price. For this reason, the interest in a cheap and easily available adsorbent for dye removal is increasing day by day. There are many researchers conducting various studies to find such an adsorbent. They come across various biological materials, both dry and wet. These include lichens, algae, tree and fruit debris, seeds and aquatic plants. The adsorbents to be used for the adsorption process should be primarily inexpensive and sufficiently efficient (Aldemir and Kul, 2020). Adsorbents made from waste rather than traditional activated carbon or materials produced by carbonization are gaining popularity as a result of rising environmental pollution. Adsorbents should also be environmentally friendly, non-toxic, easy to produce, insoluble in water, porous, with a large surface area, and scientifically recognized (Karabaş et al., 2022)

In this study, watermelon peels, which are agricultural wastes, were modified with 3 different bases and used as adsorbents to remove crystal violet dye from aqueous solutions. As a result of the modification, the adsorbent with the highest capacity was selected by considering the adsorption capacities of the adsorbents. The effect of different parameters on the adsorption mechanism was studied. The obtained results were evaluated in terms of isotherm, kinetics, and thermodynamics.

MATERIALS AND METHODS

Preparation of Adsorbents and Characterization

Watermelon used for adsorbent was purchased from a local market in Muş, Türkiye. The watermelon was cut into pieces and the insides were removed. Afterwards, the watermelon peels (WP) were dried in drying oven at 378 K. The WP that reached constant weight was grounded with laboratory blender and was sieved with 2 mm sieve. 10 grams of WP with particle size less than 2 mm was added to 3 different flasks and they were subjected to modification process by adding 250 mL 0.1M NaOH, KOH and NH_3 to the flasks. The flasks were covered with parafilm and left in a shaker for 6 hours. Then it was filtered with coarse filter paper, and until pH = 7 washed with distilled water.

The adsorbents were dried in oven at 378 K until they reached constant weight. The adsorbents were characterized by Elemental analysis, XRD, SEM and FTIR.

Preparation of crystal violet solution and batch adsorption studies

The solution of Crystal Violet (C.I. 42555, Merck) was prepared by dissolving 0.5 g (500 ppm) in 1 L of distilled water.

Adsorption isotherm experiments were performed in six different initial concentrations (100 - 350 ppm) and at three different temperatures (293, 303 and 323 K). 0.1 g adsorbent and 100 mL CV solution added to conical flasks were stirred at 210 rpm for 6 h. Three different initial concentrations were used for the adsorption kinetic experiments (100, 150 and 200 ppm). 0.5 g adsorbent and 500 mL CV solution added to the beaker were stirred at 210 rpm for 3h. The residual solutions were measured by UV-Vis.

Characterization techniques

X-ray diffraction analysis (XRD) of adsorbent was analyzed in PANalytical Empyrean equipped with X-ray generator 4 kW, spectrum range 10-80 2θ, to observe crystallization. Fourier-transform infrared spectroscopy (FTIR) analysis of adsorbent was carried out in Perkin Elmer-two spectrum Infrared Spectrophotometer equipped with resolution 1 1/cm, spectrum range 400-4000 1/cm to observe surface functional groups. Scanning electron microscope (SEM) images of adsorbent were analyzed LEO-EVO 40. Adsorption analysis were measurement with Agilent Cary 60 UV-Visible spectrophotometer device. Measurements were performed with 3mL quartz cuvettes at λmax 591 nm.

The residual solution was calculated in eq. 1.

$$q_e = \frac{C_0 - C}{w} \times V \quad (1)$$

where C and C_0 (mg/L) are equilibrium and initial liquid-phase concentrations of CV, respectively, w (g), amount adsorbent, V (L), volume of the solution.

RESULTS AND DISCUSSION

Characterization of Biosorbent

Elemental analyses of WP adsorbent show that its major constituents are 55.273% of oxygen, 37.30% of carbon, 1.346% of nitrogen, 0.027% of sulfur and 6.054% of hydrogen. This composition is comparable to the modification WP (WP+NH_3) which has 51.349% of oxygen, 41.40% of carbon, 0.945% of nitrogen, 6.28% of hydrogen and 0.026% of sulfur. This change can be interpreted by the differentiation of the structure. The atomic ratios (O+N)/C and H/C, O/C were detected to analyze polarity and aromaticity nature of adsorbent, respectively (Manisha et al., 2020). Distinctly, the decrement in all atomic ratios after a modification indicates lesser hydrophilicity and higher aromaticity compared to raw adsorbent owing to elevated removal of polar surface functional groups. Adsorbents' elemental analysis is reported in Table 1.

Table 1. Results of CHNS Analysis

	C	N	H	S	O*	O/C	H/C	(O+N)/C
WP	37.30	1.346	6.054	0.027	55.273	1.481	0.162	1.517
WP+NH_3	41.40	0.945	6.280	0.026	51.349	1.24	0.151	1.263

***** Calculated from difference

FTIR spectra of the adsorbent samples studied in the present work are illustrated in Fig. 1, A. The absorption peak at 3297 1/cm is attributed to vibrations in O-H groups. These groups are generally in the range of 3210-3660 1/cm for carboxylic acid, phenols and alcohols. The band located at about 2924 1/cm corresponds to vibrations in methylene and methyl groups. In addition, the bands at 1335 1/cm and 1420 1/cm attributed to the C-H in-plane bending vibrations in CH_3 and CH_2 groups (Yu et al., 2016). The peak around 1749 1/cm represents stretching vibrations of C=O groups (acetate groups COO, carboxylic acid, ketone, aldehyde).

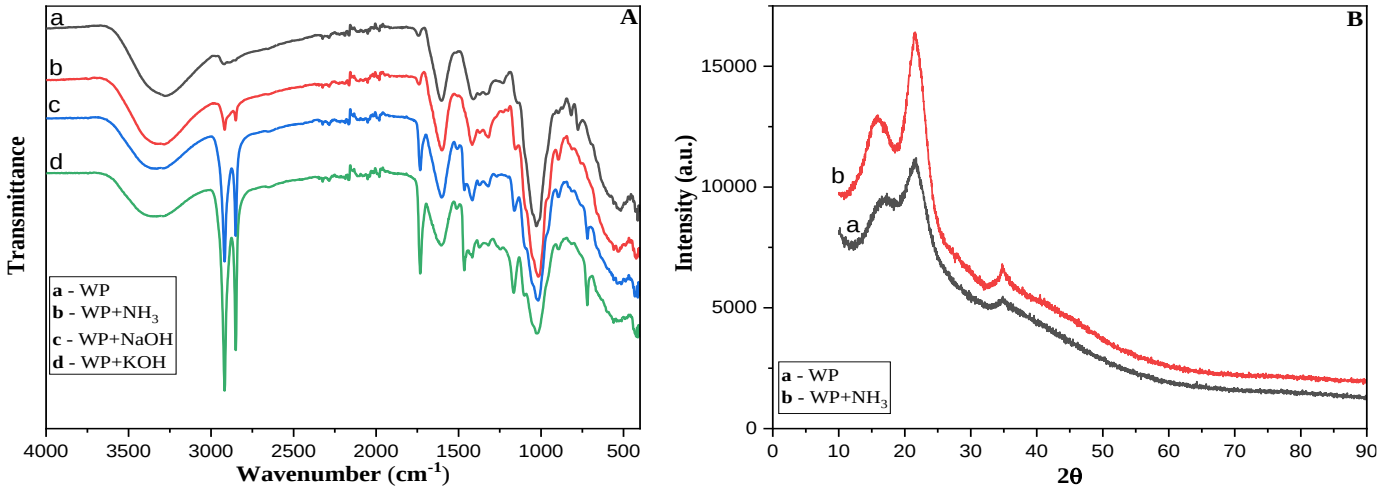

Figure 1. Different Spectrum of Adsorbents **A.** FTIR **B.** XRD

The absorption peak at 1609 1/cm represents stretching vibration bond of C=C. The peaks at 1265 1/cm and 1035 1/cm are attributed to groups of carboxylic acid, phenolic, alcoholic, ester and ether groups (Ben-Ali et. al., 2017). On the other hand, cellulose characteristic peaks generally, C-H symmetrical stretching, hydroxyl group and glycosidic bonds symmetric ring-stretching mode of polysaccharides (3310, 2900 and 900 1/cm), stretching of the C-O group of aromatic ring (1320 and 1060 1/cm), skeletal vibration of the β (1–4) glycosidic linkages (1170 and 1110 1/cm) (Zhang et al., 2018).

The XRD patterns of raw and modified WP are shown in Fig. 1, B. The WP has a less organized crystalline structure because of the various volatile and organic impurities matters present within the structure. As can be seen, two diffractograms showed the typical XRD peaks of cellulose. There are three peaks at around 15.61°, 21.89° and 34.91°, which are assigned to the reflection from the 101, 200 and 004 planes, respectively (Yu e al., 2018). However, the cellulose crystal form in the WP does not change with modification. But crystallinity in the modified WP is significantly higher than in the raw WP. The modification occurred removal of the impurity of the structure and the complete exposure of the cellulose chains. The SEM images of raw and modified WP are illustrated in Fig. 2, A, B. In raw WP, it is seen that the structure consists of amorphous, irregular, and layers. This irregularity fits the general picture of biomass. However, the structure appears to have completely changed as a result of the modification. Irregularity and layers have decreased considerably and the structure has reached a flat appearance.

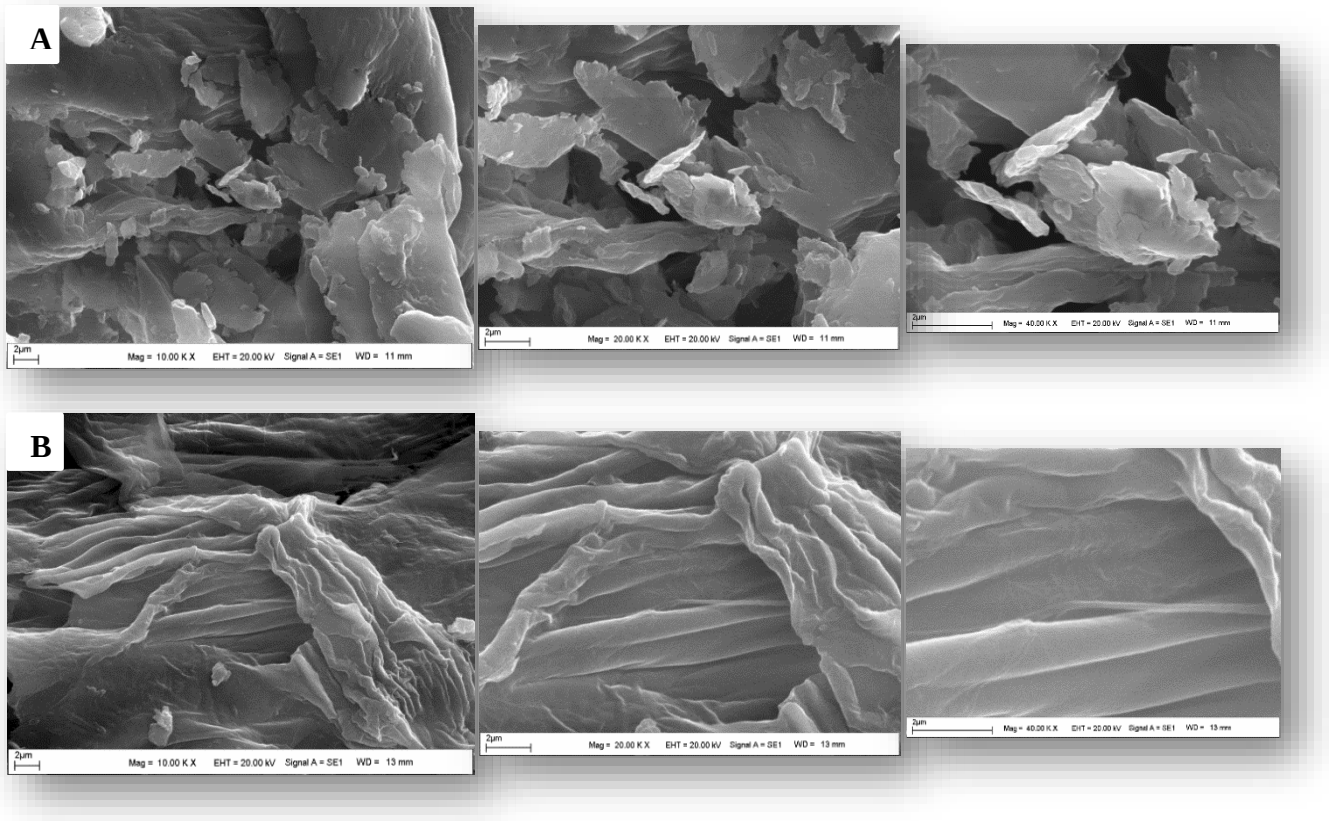

Figure 2. SEM İmages **A.** Raw WP **B.** Modified WP (WP+NH_3)

Adsorption study

Various reagents were used to increase the CV dye removal of WP. It was found that modification had a significant effect on the adsorption capacity (Fig. 3, A).

KOH, NaOH, and NH_3 were used to modify the adsorbent. Using KOH for modification did not significantly change the adsorption capacity. However, the use of NH_3 and NaOH resulted in an increase by 1.5 times. The enhancement of the alkali-treated surface can be explained by transformation of lignin structure into negative surface charges favoring the adsorption of dye molecules. In addition, increase in adsorption capacity can be due to microprecipitation of metal hydroxides (Villen-Guzman et al., 2019). On basis of the findings, NH_3 was chosen as a surface modifier.

Effect of initial concentration and contact time

The effect of initial concentration CV dye on adsorption capacity of adsorbent was determined for concentration values of 100, 150, and 200 mg/L, as shown in Fig. 3, B. Adsorption capacity of adsorbent increased from 98.4 mg/L to 176 mg/L, while initial concentration of CV dye increased from 100 mg/L to 200 mg/L. In short, increase in concentration of dye CV in solution resulted in increase in adsorption capacity of adsorbent. Initially, adsorption of CV is quite fast. About 60% of CV was adsorbed in the first 15 minutes. CV uptake increased with increasing contact time, and after 120 minutes the adsorption rate decreased significantly and the curve formed a plateau. After 180 minutes, the CV adsorption reached maximum value. The adsorption capacity at initial concentration of 100, 150 and 200 mg/L was determined to be 98.4, 136.5 and 176 mg/L, respectively. The fast initial adsorption rate may be attributed to higher number of available active sites in the form of pores and functional groups on surface of adsorbent in initial phase of the adsorption process. As adsorption

progresses, accumulation of dye molecules on surface of adsorbent impedes diffusion of molecules into pores, resulting in slow adsorption rate (Malik et al., 2007).

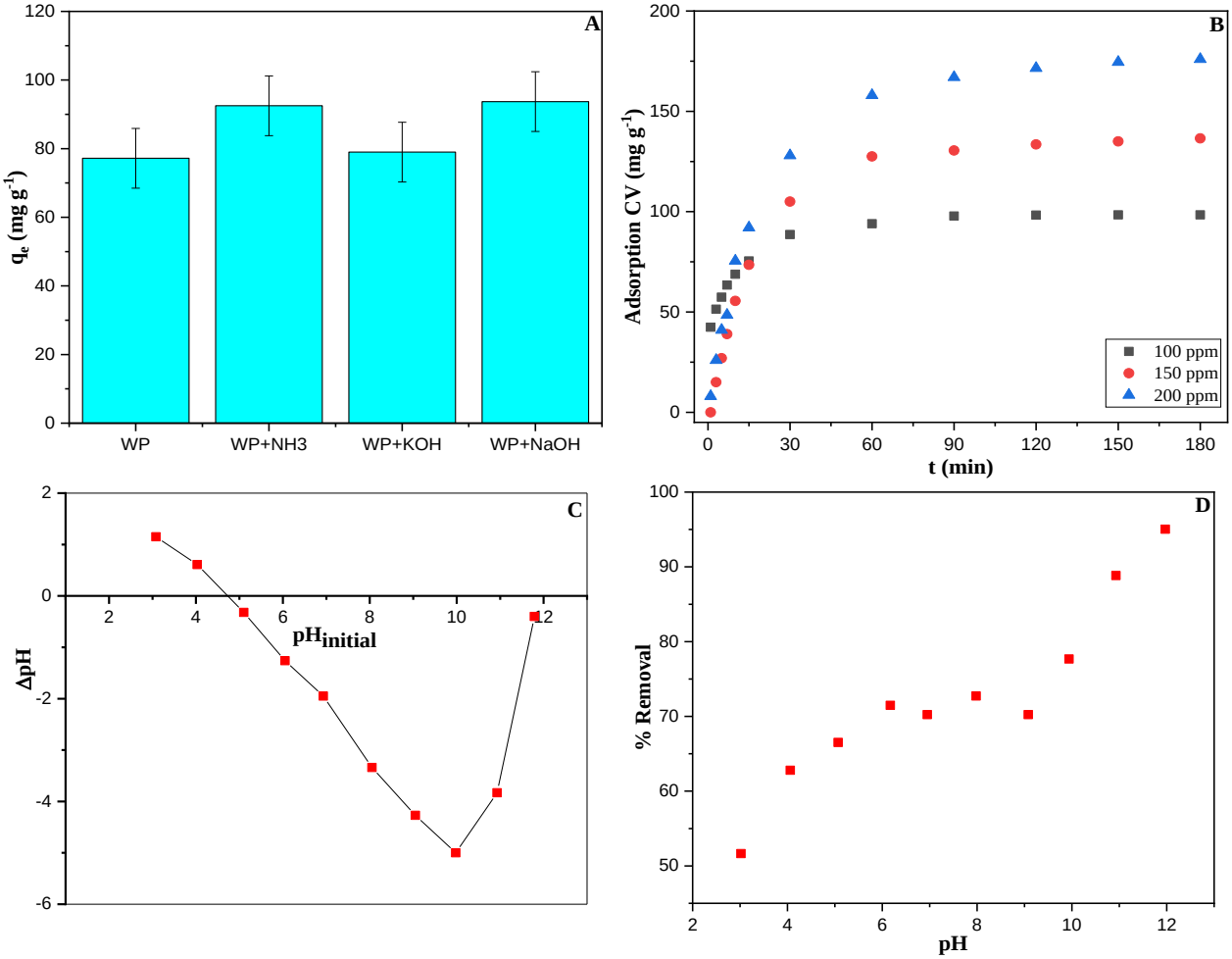

Figure 3. A. Adsorption Capacity of Adsorbents **B.** Effect of Initial Concentration and Contact Time **C.** pH_{pzc} **D.** Effect of Initial pH

Effect of initial pH

At higher pH, WP+NH_3 was found to be more effective in removing CV. Figure 3C shows the elimination of CV for a study conducted at a pH range of 3-12. At an acidic pH, the removal efficiency was lower. According to this result, positively charged CV ions are repelled by the protonation of hydroxyl and carbonyl groups on the surface of lignocellulosic material, which has a detrimental effect on removal efficiency. In contrast, the negatively charged surface of lignocellulosic material changes its charge as pH increases, making it easier to pull and remove positively charged CV ions from water. Analysis of pHpzc can be used to support this claim. The pHpzc value was determined as 4.3 (Figure 3D), so it is known that the surface of this adsorbent is positively charged below this pH (Manna et al., 2017).

Adsorption isotherms

Adsorption isotherm models, which take into account both equilibrium data and adsorption properties, describe the interaction mechanisms of pollutants and adsorbents (Al-Ghouti and Da'ana, 2020). The experimental data obtained at different temperatures (20, 30 and 50°C) were applied to Langmuir, Temkin and Freundlich Isotherm models.

Langmuir isotherm model, first developed to explain solid-gas phase adsorption on activated carbon, has recently been applied to compare and measure performance of various adsorbents. This model assumes monolayer adsorption, where adsorption may occur at fixed (finite) number of specific localized sites that are equivalent and identical, with no lateral steric interactions (Foo and Hameed, 2010).

Langmuir isotherm equation is:

$$q_e = \frac{q_m K_L C_e}{1 + K_L C_e} \quad (2)$$

Linearized form isotherm equation is:

$$\frac{C_e}{q_e} = \frac{1}{K_L q_m} + \frac{C_e}{q_m} \quad (3)$$

qe is equilibrium concentration of CV (mg/g), C_e is equilibrium concentration of CV (mg/L), q_m is max. adsorption capacity (mg/g), and K_L is Langmuir constant (L/mg).

Freundlich isotherm is oldest known model for describing reversible and nonideal adsorption, which is not limited to formation of monolayers. This model may be used to simulate multilayer adsorption with non-uniform distribution of adsorption heat and affinities across heterogeneous surface (Foo and Hameed, 2010).

The basic Freundlich isotherm equation is:

$$q_e = K_F C_e^{\frac{1}{n}} \quad (5)$$

Linearized form isotherm equation is:

$$log\ q_e = log\ K_F + \frac{1}{n} log\ C_e \quad (6)$$

1/n is adsorption intensity and K_F (mg/g) is an approximate indicator of adsorption capacity.

Temkin isotherm model first describes hydrogen adsorption on platinum electrodes (Foo and Hameed, 2010). The interactions between adsorbent and adsorbate are explicitly considered in the isotherm. The model assumes that heat of adsorption (a function of temperature) decreases linearly rather than logarithmically with coverage and ignores low and high concentration values (Erdogan, 2019).

The basic isotherm equation is:

$$q_e = B_T\ ln(A_T C_e) \quad (7)$$

Linearized form isotherm equation is:

$$q_e = B_T\ ln\ A_T + B_T\ ln\ C_e \quad (8)$$

The B_T value is calculated as follows:

$$B_T = \frac{RT}{b} \quad (9)$$

A_T (L/g) is binding constant, and B_T (J/mol) is constant related to heat of adsorption.

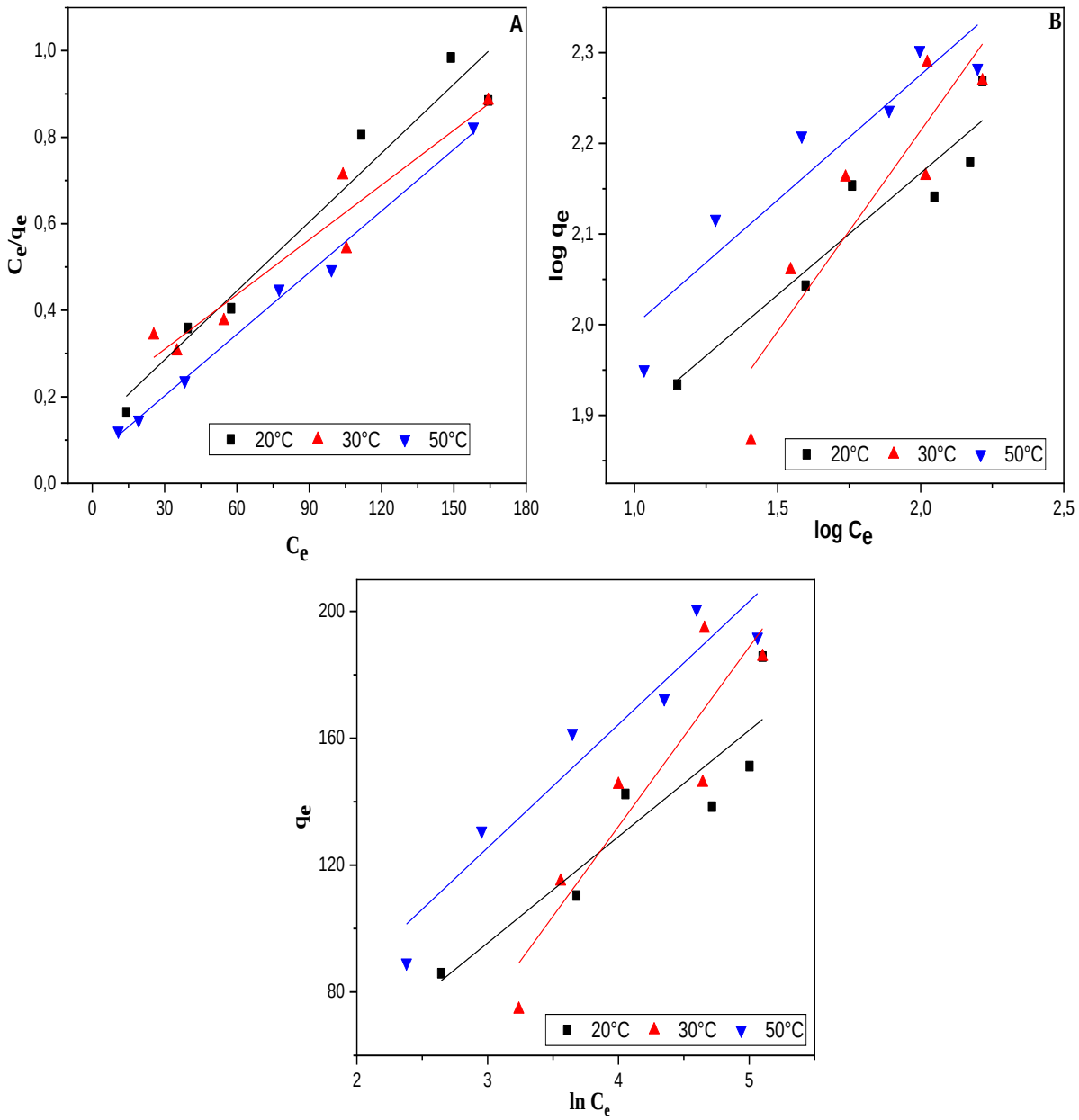

Figure 4. Isotherm Models **A.** Langmuir Model **B.** Freundlich Model **C.** Temkin Model

Table 2. Isotherm Constant

Temperature	Langmuir			Freundlich			Temkin		
	q_m	K_L	R^2	K_F	1/n	R^2	B_1	K_T	R^2
20°C	188.3	0.042	0.95	42.5	0.268	0.89	33.5	-	0.84
30°C	236.9	0.023	0.92	21.2	0.442	0.81	56.5	-	0.83
50°C	210.5	0.079	0.99	52.7	0.276	0.88	38.8	1.26	0.91

The regression coefficients and values of constants for isotherm models were obtained from the diagram shown in Fig. 4, and values of the constants were given in Table 2. All data obtained show that the study fit Langmuir more than Temkin and Freundlich models. According to Langmuir isotherm, the maximum value of q_m was determined to be 236.9 mg/g at T = 30°C. Although the maximum q_m increased from 188.3 to 236.9 mg/g, the temperature was increased from 20°C to 30°C, the q_m decreased from 236.9 to 210.5 mg/g when the temperature was increased from 30°C to 50°C.

The increase in adsorption capacity with increasing temperature confirmed that adsorption is endothermic process. The adsorption capacity increasing with temperature proves that this process is an endothermic process. Nevertheless, at high temperatures, there may have been a decrease in adsorption capacity due to decomposition of biomolecule. The regression coefficients (R^2) show to be quite reasonable at all temperatures studied. The highest R^2 was calculated as 0.99 at T = 50°C.

Adsorption kinetics

Pseudo-first order model (PFO) and pseudo-second-order model (PSO), were used to study adsorption kinetics of CV on an adsorbent.

PFO model equation applies to adsorption in liquid-solid system. It assumes that adsorbate uptake is directly proportional to difference in the degree of saturation of concentration (Emmanuel et al., 2020). The equation of PFO model is termed as follows:

$$\frac{dq_t}{dt} = k_1(q_e - q_t) \tag{10}$$

Linearized form equation is:

$$log\ (q_e - q_t) = Iog\ q_e - k_1 t \tag{11}$$

The plot of ln(q_e-qt) versus t is used to calculate q_e and k_1 from the intercept and slope respectively (Fig. 5, A).

q_e (mg/L) is the equilibrium concentration of CV on adsorbent and q_t (mg/g) is concentration of CV at time. k_1 is the PFO constant (1/min).

PSO model is based on chemisorption. The adsorbent and adsorbate form covalent bond (Wang and Guo, 2020). The equation of PSO model is expressed as follows:

$$\frac{dq_t}{dt} = k_2(q_e - q_t)^2 \tag{12}$$

Linearized form equation is:

$$\frac{t}{q_t} = \frac{1}{k_2 q_e^2} + \frac{t}{q_e} \tag{13}$$

The plot of t/qt versus t is used to calculate q_e and k_2 from intercept and slope respectively (Fig. 5, B). k_2 is the PSO constant (1/min).

The kinetic diagrams generated with the obtained data are shown in Figure 5. The data for the PFO and PSO models are shown in Table 3. The results show that the adsorption process of dye MB follows PSO model since R^2 values are higher compared to PFO models. Moreover, the q_e values calculated with PSO and the experimental q_e values are similar. The results show that a chemisorption process regulates the adsorption of the dye CV by the WP+NH_3.

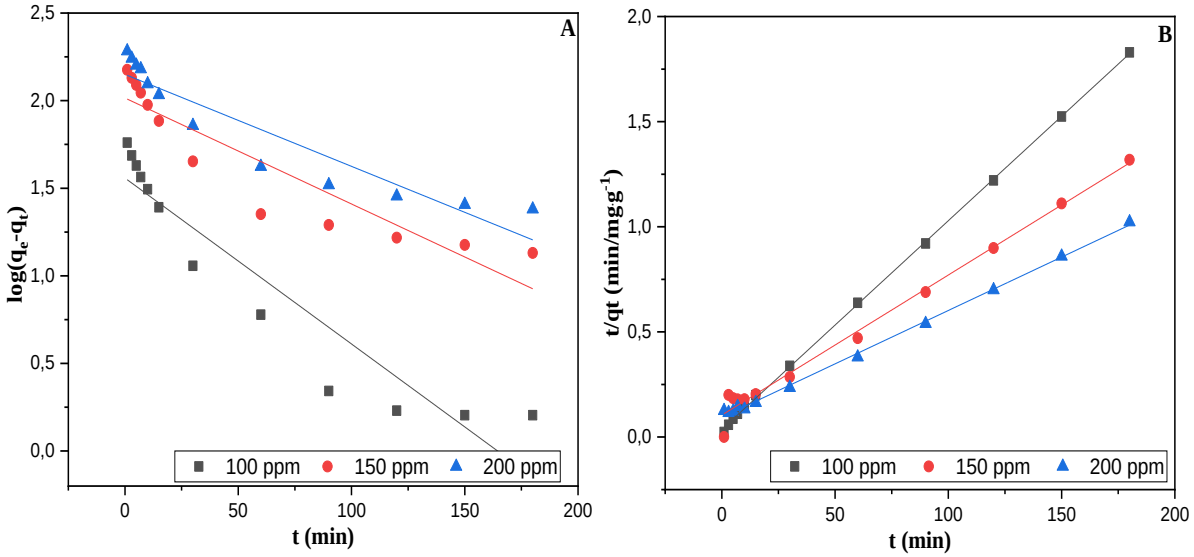

Figure 5. Kinetic Models **A.** Pseudo First Order Model **B.** Pseudo Second Order Model

Table 3. Kinetic Constant of PFO and PSO

T°C	C_0	PFO			PSO		
		k_1	q_e	R^2	k_2	q_e	R^2
20°C	100	0.009	4.74	0.89	0.257	111.1	0.99
20°C	150	0.006	7.49	0.85	0.057	166.6	0.98
20°C	200	0.005	8.57	0.88	0.053	200	0.99

Thermodynamics

The energy of an isolated system is constant from a thermodynamic point of view. It can neither be gained nor lost, and the only driving force is entropy change. Both enthalpy and energy values must be considered to determine which process will occur spontaneously (Wibowo et al., 2017). Changes in standard entropy (S°), standard enthalpy (H°) and standard free energy (G°) are thermodynamic parameters that must be considered to detect the adsorption processes. Thermodynamic parameters, ΔG°, ΔS° and ΔH° may be calculated by substituting Eq. (14) with Eq. (15).

$$\Delta G° = -RT \ln K_c \quad (14)$$

$$\ln K_c = \frac{\Delta S^0}{R} - \frac{\Delta H^0}{RT} \quad (15)$$

$$K_c = q_e/C_e \quad (16)$$

K_C thermodynamic equilibrium constant (dimensionless); T (Kelvin) is temperature and R (8.314 J/Kmol) is universal gas constant. According to Eq. 15, ln K_C versus 1/T is plotted and were calculated ΔH° and ΔS° from this graph. Thermodynamic calculations are given in Table 3.

Table 3 displays obtained values of ΔG°, ΔH°, and ΔS° as thermodynamic parameters used to identify adsorption process characteristics. ΔG° value of the adsorption process is -2.497, -2.987, and -5.151 kJ/mol at 20, 30, and 50 °C, respectively.

Table 3. Thermodynamic Parameters for Adsorption

T (°C)	ΔG^0 (kJ/mol)	ΔS^0 (kJ/mol)	ΔH^0 (kJ/mol K)
20°C	-2.497		
30°C	-2.987	0.0307	0.0025
50°C	-5.151		

Negative ΔG° value indicates that adsorption of CV dye on adsorbent surface occurs spontaneously under the conditions of the experiment. We can see that the ΔG° value shifts from negative to more negative with increasing temperature. This indicated adsorption process at higher temperatures is more favourable and feasible than at low temperatures (Wibowo et al., 2017). In this work, ΔH° value determined is also positive, i.e., 0.0025 kJ/mol. Positive ΔH° value shows endothermic adsorption process (Ali et al., 2022). Sign of ΔS° indicates whether arrangement of adsorbate at solid/gas interface during adsorption process is more random (ΔS°>0) or less random (ΔS°<0). In this work, ΔS° value determined is also positive, i.e., 0.0307 kJ/mol. The positive ΔS° value shows a more random adsorption process (Mudzielwana et al., 2019).

CONCLUSION

In summary, adsorbents were obtained from watermelon peels. Watermelon peels provide higher adsorption of crystal violet with NH3 and NaOH modification. NH3 modification was used as an adsorbent in the study. After modification, the structural changes were determined by SEM, XRD, FTIR, and elemental analysis. The experimental data indicated a good correlation between pseudo-second-order model and Langmuir isotherms models. Adsorption capacity (Langmuir q_{max}) is 236.9 mg/g at 50 °C. The thermodynamic study shows that adsorption is spontaneous, random and endothermic. (ΔS°>0, ΔG°<0, ΔH°>0). Consequently, this inexpensive adsorbent appears to perform well in removing crystal violet.

ACKNOWLEDGEMENTS

This project is funded by TUBITAK 2209-A program.

Conflict of Interest

The article authors declare that there is no conflict of interest between them.

Author's Contributions

The authors declare that they have contributed equally to the article.

REFERENCES

Aldemir, A., Kul, A. R. (2020). Isotherm, kinetic and thermodynamic studies for the adsorption of methylene blue on almond leaf powder. *Cumhuriyet Science Journal*, 41(3), 651-658. https://doi.org/10.17776/csj.720332.

Al-Ghouti, M.A., Da'ana, D.A., (2020). Guidelines for the use and interpretation of adsorption isotherm models: A review. *Journal of Hazardous Materials*, 393, 122383. https://doi.org/10.1016/j.jhazmat.2020.122383.

Ali, N.S., Jabbar, N.M., Alardhi, S.M., Majdi, H.S., Albayati, T.M. (2022). Adsorption of methyl violet dye onto a prepared bio-adsorbent from date seeds: isotherm, kinetics, and thermodynamic studies, *Heliyon*, 8(8), e10276. https://doi.org/10.1016/j.heliyon.2022.e10276.

Bayram, O., Moral, E., Göde, F. (2023). Removal of Crystal Violet Dye from Aqueous Solution Using Biochar Obtained from Oleaster Seeds. *Journal of the Institute of Science and Technology,*13(1), 448-457. https://doi.org/10.21597/jist.1170769

Ben-Ali, S., Jaouali, I., Souissi-Najar, S., Ouederni, A. (2017). Characterization and adsorption capacity of raw pomegranate peel biosorbent for copper removal. *Journal of Cleaner Production*, 142(4), 3809-3821. https://doi.org/10.1016/j.jclepro.2016.10.081.

Dinçer, A. Sevildik, M., Aydemir, T. (2019). Optimization, isotherm and kinetics studies of azo dye adsorption on eggshell membrane. *International Journal of Chemistry and Technology*, 3(1), 52-60. https://doi.org/10.32571/ijct.538736.

Fatma O. E. (2019). Freundlich, Langmuir, Temkin, DR and Harkins-Jura Isotherm Studies on the Adsorption of CO_2 on Various Porous Adsorbents. *International Journal of Chemical Reactor Engineering*, 17(5), 20180134. https://doi.org/10.1515/ijcre-2018-0134.

Foo, K.Y., Hameed, B.H., Insights into the modeling of adsorption isotherm systems, *Chemical Engineering Journal*, 156(1), 2-10. https://doi.org/10.1016/j.cej.2009.09.013.

Güneş, D.S. (2020). Removal of Maxilon Golden Yellow GL EC 400% from the Wastewater by Adsorption Method Using Different Clays. *Sakarya University Journal of Science*, 24(5), 1081-1093. https://doi.org/10.16984/saufenbilder.526957.

Gürses, A. Güneş, K., Şahin, E. (2021). Chapter 5 - Removal of dyes and pigments from industrial effluents, In Advances in Green and Sustainable Chemistry, Elsevier, 135-187. https://doi.org/10.1016/B978-0-12-817742-6.00005-0.

Heidarinejad, Z., Dehghani, M.H., Heidari, M., Javedan G., Imran, A., Sillanpää, M., (2020). Methods for preparation and activation of activated carbon: a review. *Environ. Chem. Lett.* 18, 393–415. https://doi.org/10.1007/s10311-019-00955-0.

Karabaş, B., Keskinkan, O., Sarı, B., Yeşiltaş, H. Kıvanç, E., Çağatayhan, B. (2022). The usage of palm (Washingtonia filifera) fibers for the removal of crystal violet from synthetic dye solution by adsorption. *International Journal of Chemistry and Technology*, 6(1), 66-75. https://doi.org/10.32571/ijct.1131313.

Kul, A.R., Aldemir, A., Elik, H. (2019). Adsorption of Acid Blue 25 on peach seed powder: Isotherm, kinetic and thermodynamic studies. *Environmental Research and Technology*, 2(4), 233-242. https://doi.org/10.35208/ert.650398

Malik, R., Ramteke, D.S., Wate, S.R. (2007). Adsorption of malachite green on groundnut shell waste based powdered activated carbon. *Waste Manag.*, 27, 1129–1138. https://doi.org/10.1016/j.wasman.2006.06.009.

Manisha, C., Rahul, K., Sudarsan, N. (2020). Activated biochar derived from Opuntia ficus-indica for the efficient adsorption of malachite green dye, Cu^{+2} and Ni^{+2} from water, *Journal of Hazardous Materials*, 392, 122441. https://doi.org/10.1016/j.jhazmat.2020.122441.

Manna, S., Roy, D., Saha, P., Gopakumar, D., Thomas, S. (2017). Rapid methylene blue adsorption using modified lignocellulosic materials. *Process Safety and Environmental Protection*, 107, 346-356. https://doi.org/10.1016/j.psep.2017.03.008.

Mudzielwana, R., Gitari, M.W., Ndungu, P. (2019). Performance evaluation of surfactant modified kaolin clay in As(III) and As(V) adsorption from groundwater: adsorption kinetics, isotherms and thermodynamics, *Heliyon*, 5(11), e02756. https://doi.org/10.1016/j.heliyon.2019.e02756.

Öter, Ç. (2021). Bioadsorbent Efficiency in Heavy Metal Removal from Aqueous Solutions: Adsorption Kinetics, Isotherm, and Thermodynamics. *Hittite Journal of Science and Engineering*, 8(4), 313-320. https://doi.org/10.17350/HJSE19030000244

Revellame, E.D. Fortela, D.L., Sharp, W., Hernandez, R., Zappi, M.E. (2020). Adsorption kinetic modeling using pseudo-first order and pseudo-second order rate laws: A review. *Cleaner Engineering and Technology*, 1, 100032. https://doi.org/10.1016/j.clet.2020.100032.

Villen-Guzman, M., Gutierrez-Pinilla, D., Gomez-Lahoz, C., Vereda-Alonso, C., Rodriguez-Maroto, J.M., Arhoun, B. (2019). Optimization of Ni (II) biosorption from aqueous solution on modified lemon peel, Environmental Research, 179, 108849. https://doi.org/10.1016/j.envres.2019.108849.

Wang, J., Guo, X. (2020). Adsorption kinetic models: Physical meanings, applications, and solving methods. *Journal of Hazardous Materials*, 390, 122156. https://doi.org/10.1016/j.jhazmat.2020.122156.

Wibowo, E., Rokhmat, M., Khairurrijal, S., Abdullah, M. (2017). Reduction of seawater salinity by natural zeolite (Clinoptilolite): Adsorption isotherms, thermodynamics and kinetics, *Desalination*, 409, 146-156. https://doi.org/10.1016/j.desal.2017.01.026.

Yu, Q., Li, M., Ji, X., Qiu, Y., Zhu, Y., Leng, C. (2016). Characterization and methanol adsorption of walnut-shell activated carbon prepared by KOH activation. *J. Wuhan Univ. Technol.-Mat. Sci. Edit*. 31, 260–268. https://doi.org/10.1007/s11595-016-1362-3

Yu, X., Bao, X., Zhou, C., Zhang, L., El-Gasim, A., Yagoub, A., Yang, H., Ma, H., (2018). Ultrasound-ionic liquid enhanced enzymatic and acid hydrolysis of biomass cellulose, *Ultrasonics Sonochemistry*, 41, 410-418. https://doi.org/10.1016/j.ultsonch.2017.09.003.

Zhezi, Z., Mingming, Z., Dongke, Z., (2018). A Thermogravimetric study of the characteristics of pyrolysis of cellulose isolated from selected biomass. *Applied Energy*, 220, 87-93. https://doi.org/10.1016/j.apenergy.2018.03.057.